Conversion of Tyr361β to Leu in Mammalian Protein Farnesyltransferase Impairs Product Release but Not Substrate Recognition†

Rebecca A. Spence,‡ Kendra E. Hightower,‡ Kimberly L. Terry,§ Lorena S. Beese,§ Carol A. Fierke,§,|| and Patrick J. Casey*,‡,§

Departments of Pharmacology and Cancer Biology and Biochemistry, Duke University Medical Center, Durham, North Carolina 27710

Received May 15, 2000; Revised Manuscript Received September 6, 2000

ABSTRACT: Protein farnesyltransferase catalyzes the lipid modification of protein substrates containing Met, Ser, Gln, or Ala at their C-terminus. A closely related enzyme, protein geranylgeranyltransferase type I, carries out a similar modification of protein substrates containing a C-terminal Leu residue. Analysis of a mutant of protein farnesyltransferase containing a Tyr-to-Leu substitution at position 361 in the β subunit led to the conclusion that the side chain of this Tyr residue played a major role in recognition of the protein substrates. However, no interactions have been observed between this Tyr residue and peptide substrates in the crystal structures of protein farnesyltransferase. In an attempt to reconcile these apparently conflicting data, a thorough kinetic characterization of the Y361L variant of mammalian protein farnesyltransferase was performed. Direct binding measurements for the Y361L variant yielded peptide substrate binding that was actually some 40-fold tighter than that with the wild-type enzyme. In contrast, binding of the peptide substrate for protein geranylgeranyltransferase type I was very weak. The basis for the discrepancy was uncovered in a pre-steady-state kinetic analysis, which revealed that the Y361L variant catalyzed farnesylation of a normal peptide substrate at a rate similar to that of the wild-type enzyme in a single turnover, but that subsequent turnover was prevented. These and additional studies revealed that the Y361L variant does not "switch" protein substrate specificity as concluded from steady-state parameters; rather, this variant exhibits severely impaired product dissociation with its normal substrate, a situation resulting in a greatly compromised steady-state activity.

Protein farnesyltransferase (FTase)[1] catalyzes the transfer of a 15-carbon farnesyl isoprenoid from farnesyl diphosphate (FPP) to a conserved cysteine of its protein substrate forming a thioether bond (*1*, *2*). The reactive cysteine is located in the C-terminal CaaX motif in which C is the modified cysteine, a is often an aliphatic residue, and X is Ser, Met, Ala, or Gln. Farnesylation mediates membrane localization and possibly protein−protein interactions of a variety of proteins involved in cellular regulatory events (*3*−*5*). The farnesylation of Ras proteins in particular has received much attention since the discovery that oncogenic forms of these proteins require modification to be able to transform cells (*6*, *7*). A closely related enzyme, protein geranylgeranyltransferase type I (GGTase-I), also catalyzes the prenylation of CaaX-containing proteins (*8*). However, this enzyme transfers a 20-carbon geranylgeranyl group from geranylgeranyl diphosphate to protein substrates with a Leu residue in the X position of the CaaX motif (*9*, *10*). Known targets of GGTase-I include most γ subunits of heterotrimeric G proteins and Ras-related GTPases such as members of the Rac/Rho family (*1*, *8*). In addition to proteins, short peptides containing the appropriate CaaX sequences can be used as efficient substrates by both protein prenyltransferases (*10*, *11*).

Both FTase and GGTase-I are heterodimers; they share an identical α subunit but possess distinct β subunits whose sequences are significantly similar (*11*−*13*). Both prenyltransferases are zinc metalloenzymes in which the metal ion plays a catalytic role (*14*−*17*). In FTase, this zinc atom is located in the β subunit near the α/β subunit interface and marks the location of the active site (*18*). The β subunit is folded into an α/α barrel whose central cavity provides a deep hydrophobic cleft along one side to which the isoprenoid moiety of FPP binds (*19*). Structures of FTase complexed with both inactive FPP analogues and a CaaX peptide revealed that the bound peptide in the central cavity displays contacts to both the enzyme and the FPP molecule, and the cysteine sulfur of the peptide coordinates the active site zinc ion (*20*, *21*). However, the relatively large distance (7 Å) between the cysteine sulfur and C_1 of FPP indicates

† This work was supported by NIH Grants GM46372 (P.J.C.), GM40602 (C.A.F.), and GM52382 (L.S.B.). R.A.S. was the recipient of a fellowship from the Leukemia Society of America.

* To whom correspondence should be addressed: Department of Pharmacology and Cancer Biology, Box 3813, Duke University Medical Center, Durham, NC 27710. Telephone: (919) 613-8613. Fax: (919) 613-8642. E-mail: casey006@mc.duke.edu.

‡ Department of Pharmacology and Cancer Biology.

§ Department of Biochemistry.

|| Current address: Department of Chemistry, University of Michigan, Ann Arbor, MI 48109.

[1] Abbreviations: FTase, protein farnesyltransferase; FPP, farnesyl diphosphate; CaaX, sequence motif of proteins consisting of an invariant Cys residue fourth from the C-terminus; GGTase-I, protein geranylgeranyltransferase type I; GCVLS, pentapeptide Gly-Cys-Val-Leu-Ser; TKCVIL, hexapeptide Thr-Lys-Cys-Val-Ile-Leu; [^{3}H]FPP, tritium-labeled FPP; [^{32}P]FPP, FPP labeled with ^{32}P; *I*, {(*E*,*E*)-2-[oxo[(3,7,11-trimethyl-2,6,10-dodecatrienyl)oxy]amino]phosphonic acid}; TLC, thin-layer chromatography; TCEP, tris(2-carboxyethyl)phosphine hydrochloride.

10.1021/bi001084r CCC: $19.00
Published on Web 10/21/2000

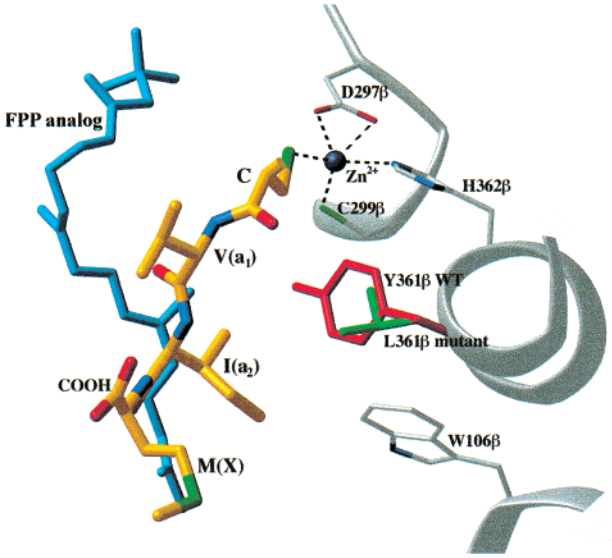

FIGURE 1: Complex of rat FTase with the FPP analogue *I* (cyan) and the four C-terminal residues of a K-Ras4B-derived peptide, CVIM (yellow). Residue Y361 in the β subunit (red) is 3.7 Å from the CaaX peptide substrate at its closest point of contact. A model of the Y361L variant (green) that contains the only Leu rotamer that does not result in a steric clash with residue W106 is shown; at its closest point, the Leu rotamer is 4.3 Å from the CaaX peptide. Also shown are the essential zinc ion (dark blue) and its ligands (gray). The coordinates are deposited in the Protein Data Bank as entry 1D8D.

that further rearrangements of one or both substrates are necessary for product formation to occur.

Analysis of the kinetic pathway indicates that FTase proceeds through a functionally ordered mechanism in which FPP binds first to the enzyme (*22*, *23*), with the overall equilibrium dissociation constant of FPP in the low nanomolar range. The protein substrate binds to the E·FPP complex in a fashion that is essentially irreversible (*23*, *24*). The zinc ion is required for both protein substrate binding and enzymatic activity (*14*, *15*). Both spectroscopic analysis of Co^{2+}-substituted FTase (*17*) and crystallographic analyses of enzyme−substrate complexes (*20*, *21*) indicate that the metal is directly involved in coordinating the cysteine sulfur in the CaaX motif of the protein substrate. The chemical step of catalysis is $>10\ s^{-1}$ (*17*, *23*, *24*), i.e., some 200-fold faster than the steady-state turnover rate, which is limited by product dissociation from the enzyme (*23*). In what is thought to be an important component in the overall kinetic mechanism, the binding of additional substrate (either FPP or protein/peptide) is necessary to trigger release of the product from the enzyme (*25*).

In addition to structural data, site-directed mutagenic studies of FTase from rats, humans, and yeast have begun to identify residues that affect substrate binding, specificity, and catalytic activity (*26*−*31*). Mutants in the β subunit of yeast FTase were identified by random screening for enzyme variants that exhibited relaxed specificity toward protein substrates (*29*). Steady-state kinetic analysis of one such mutant of FTase in which Tyr362 (which corresponds to Tyr361 in mammalian FTase) was changed to a Leu residue showed that the steady-state ability of the Y362L variant to farnesylate a GGTase-I substrate protein (i.e., where the X residue was Leu) was improved approximately 20-fold relative to that of wild-type FTase (*29*). The authors concluded that introducing a distinct amino acid change at position 362 switched the substrate specificity of FTase to that of GGTase-I, and therefore, the side chain of Tyr362 played a major role in recognition of the protein CaaX sequence. A very recent report indicates that introducing the corresponding Tyr-to-Leu substitution (i.e., at Tyr361) into the human FTase yielded similar results (*32*). Surprisingly, however, the available crystal structures of ternary complexes of FTase place this residue at the opening of the hydrophobic cleft, and no interactions were observed between this specific Tyr and peptide substrates (*20*, *21*) (see Figure 1); the one other mutagenesis study directly addressing substrate selectivity identified a quite different region of the β subunit as being important in this regard (*30*).

In an attempt to reconcile the apparently conflicting data with regard to the role of Y361 in substrate selectivity, and to explore the potential mechanism through which the Y361L variant might be "converted" to an enzyme preferring substrates of GGTase-I, we performed a thorough biochemical characterization of the Y361L variant of mammalian FTase. Initial steady-state results indicated that the Y361L variant could not efficiently catalyze the farnesylation of the FTase peptide substrate, GCVLS, yet exhibited a measurable activity with the GGTase-I peptide substrate, TKCVIL. However, transient kinetic analysis revealed that the Y361L variant could in fact catalyze farnesylation of the peptide substrate GCVLS with a rate constant similar to that of the wild-type enzyme in a single turnover, but that subsequent turnover of the GCVLS peptide was inhibited. These and additional studies, including direct binding measurements with the peptide substrates, revealed that the Y361L variant does not switch protein substrate specificity as concluded from steady-state parameters; rather, this variant exhibits severely impaired product dissociation with its normal substrate, a situation resulting in a severely compromised k_{cat} measured by steady-state methods.

EXPERIMENTAL PROCEDURES

Miscellaneous. Tritium-labeled FPP ([^{3}H]FPP) was purchased from NEN Life Science Products (Boston, MA), and unlabeled FPP was purchased from BioMol (Plymouth Meeting, PA). FPP labeled with ^{32}P ([^{32}P]FPP) was synthesized as described previously (*33*). Dansyl-labeled peptides, dansyl-GCVLS and dansyl-GAVLS, and the GGTase-I substrate peptide, TKCVIL, were synthesized by Applied Analytical, Inc. (Chapel Hill, NC), while the FTase substrate peptide, GCVLS, was prepared by Quality Controlled Biochemicals, Inc. (Hopkinton, MA). All peptides were purified by reverse-phase HPLC prior to use. Peptide concentrations were determined by the titration of thiols with 5,5′-dithiobis(2-nitrobenzoate) (*34*). The FPP analogue {(*E*,*E*)-2-[oxo[(3,7,11-trimethyl-2,6,10-dodecatrienyl)oxy]amino]-phosphonic acid}, termed *I*, was obtained from Calbiochem (San Diego, CA). Silica G60 thin-layer chromatography (TLC) plates were purchased from Whatman Inc. and EM Science. Recombinant H-Ras protein was produced via bacterial expression and purified as described previously (*11*). Protein concentrations were determined by the Coomassie Blue binding method using a commercial kit (Bio-Rad, Hercules, CA). The reducing agent tris(2-carboxyethyl)-phosphine hydrochloride (TCEP) was purchased from Pierce

(Rockford, IL). Standard molecular biology methods were employed for subcloning and sequencing.

Site-Directed Mutagenesis. Site-specific mutations were introduced into the β subunit of FTase using the QuikChange Site-Directed mutagenesis kit (Stratagene). The cDNA of the FTase β subunit contained within the pET28a vector (Novagen) was previously prepared (*35*). A double-base mutation (TAC $\rightarrow$ CTC) was introduced, producing the amino acid change of Tyr361 to Leu (Y361L), and the altered cDNA was sequenced using the Sequenase Version 2.0 DNA sequencing kit (United States Biochemical). The confirmed mutant cDNA was then subcloned by replacing a fragment of the wild-type β with a fragment containing the altered cDNA into the pET23a/PFT vector described previously (*36*). The resulting pET23a/PFT-Y361L vector contained both the wild-type α and altered β subunits of FTase.

Production and Purification of Wild-Type and Mutant FTases. Production of recombinant bacterial FTases and their purification were performed as previously described (*36*). During purification, FTase assays were performed using a well-documented filter binding assay (*11*). H-Ras protein (which contains the CaaX sequence CVLS) was used as a substrate for wild-type FTase; the same substrate yielded no significant product formation when used to follow purification of the Y361L mutant. To identify the fractions containing active Y361L, an H-Ras protein whose C-terminal amino acid residue had been changed from Ser to Leu (Ras-CVLL) was used as a substrate (*9*). Following the final chromatographic step using Phenyl-Sepharose HP resin (Pharmacia), fractions containing purified FTase were pooled, concentrated to a protein concentration of >1 mg/mL, flash-frozen in liquid nitrogen, and stored at -80 °C until they were used.

Measurement of the FPP Binding Affinity. FPP binding affinities of wild-type and Y361L FTase were measured by equilibrium dialysis as previously described (*36*). Briefly, a dialysis chamber (Scienceware, Pequannock, NJ) was used in which 5 $\times$ 2 mL wells were divided by a dialysis membrane. Each of the wells on one side of the dialysis membrane contained 1 mL of [^{3}H]FPP (20 nM, 20 Ci/mmol) in 50 mM Heppso/NaOH (pH 7.8) and 1 mM TCEP; the other side of the well contained varying concentrations of enzyme in the same equilibration buffer. Initial assays showed that 20 h at 25 °C was sufficient to bring the solution in the two wells to equilibrium and that the enzyme was stable during this time period. Once equilibrium was attained, aliquots were removed from each side of the membrane and the radioactivity was determined by scintillation counting. The concentration of free FPP ($[FPP]_{free}$) was determined by the amount of radioactivity in the FPP chamber, and the concentration of total FPP ($[FPP]_{tot}$) was determined by the amount of radioactivity in the enzyme chamber. The difference between the two concentrations is equal to the amount of enzyme-bound FPP ([E·FPP]). The FPP equilibrium dissociation constants, K_d, were then calculated on the basis of a nonlinear least-squares fit of the data using eq 1.

$$\frac{[E\cdot FPP]}{[FPP]_{tot}} = \frac{[E]_{free}}{K_d + [E]_{free}} \quad (1)$$

Measurement of the Peptide Affinity for the FTase·I Complex. The equilibrium dissociation constant for dansyl-GCVLS binding to a FTase·isoprenoid complex was determined from the increase in fluorescence of the dansyl group as the dansyl-labeled peptide binds to the enzyme complex (*37*). Binary complexes were formed by preincubating either wild-type FTase or the Y361L variant (each at 0.02 μM) with the nonsubstrate FPP analogue *I* (at 0.2 μM) in a 3 mL cuvette at 25 °C for >5 min. The incubation buffer consisted of 50 mM Bes/NaOH (pH 7.0), 1 mM $MgCl_2$, 0.01 μM EDTA, and 2 mM TCEP with an ionic strength maintained at 0.1 M with NaCl. Dansyl-labeled peptides were titrated into the FTase·*I* complex solution; the solution was allowed to equilibrate for 5 min after each addition of peptide, and the fluorescence was then determined. Tryptophan residues of FTase were excited at 280 nm, and the emission of the dansyl group due to energy transfer from the enzyme to the bound dansyl-labeled peptide was read at 496 nm (Perkin-Elmer LS50B, slit widths of 10 nm). Fluorescence changes observed from the titration of the control peptide dansyl-GAVLS were subtracted as background. The K_d of dansyl-GCVLS was calculated using eq 2 (*38*):

$$FL = IF + \frac{EP - IF}{2[E]}[([E] + [Dns] + K_d) - \sqrt{([E] + [Dns] + K_d)^2 - 4[E][Dns]}] \quad (2)$$

where FL is the fluorescence corrected for background, EP is the fluorescence end point, IF is the initial fluorescence, [E] is the concentration of enzyme, [Dns] is the concentration of dansyl-GCVLS, and K_d is the dissociation constant for dansyl-GCVLS.

Binding affinities of GCVLS and TKCVIL were determined using a competition assay by monitoring the decrease in fluorescence resulting from titration of the competing peptide (*37*). Peptide GCVLS or TKCVIL were titrated into a solution containing the appropriate FTase (at 0.02 μM), the *I* analogue (at 0.2 μM), and dansyl-GCVLS (at 0.12 μM for wild-type FTase and 0.25 μM for the Y361L variant) under the conditions described above. The resulting decrease in the dansyl fluorescence was fit to eq 3:

$$FL = \frac{IF}{1 + (K_{d,dns}/[Dns])(1 + [Pep]/K_{d,pep})} + EP \quad (3)$$

where FL is the observed fluorescence corrected for background, IF is the initial fluorescence, EP is the fluorescence end point, $K_{d,dns}$ is the dissociation constant of the dansyl-GCVLS determined previously, [Dns] is the concentration of the dansyl-GCVLS, [Pep] is the concentration of the added peptide, and $K_{d,pep}$ is the dissociation constant for the competing peptide.

Determination of Steady-State Parameters. The K_m and k_{cat} values for peptide substrates were determined by quantifying the amount of ^{3}H transferred from [^{3}H]FPP to the peptide substrate (GCVLS or TKCVIL) as described previously (*35*). Alternatively, [^{32}P]FPP was used as the isoprenoid substrate, and product formation was assessed and quantified by measuring the extent of $^{32}PP_i$ formation by TLC. In either assay, saturating amounts of [^{3}H]FPP (1 μM, 8$-$15 Ci/mmol) or [^{32}P]FPP (1 μM, 1.5 Ci/mmol) and varying amounts of peptide substrate (0$-$1 mM) were added to assay buffer consisting of 50 mM Heppso/NaOH (pH 7.8), 5 mM $MgCl_2$, 1 mM TCEP, 5 μM $ZnCl_2$, and 0.2% octyl

glucoside that was pre-equilibrated at 25 °C. Reactions were initiated by addition of FTase (10 nM final concentration, either wild-type or Y361L) in a total volume of 50 μL. Aliquots (5 μL) were removed at designated times and reactions quenched with an equal volume of 1 mM HCl in 80% 2-propanol. Reactions were allowed to proceed to no more than 10% completion and followed typical Michaelis−Menten-type kinetics. Mixtures whose reactions had been quenched were spotted onto aluminum-backed TLC plates (silica gel 60) and subsequently developed with a 2-propanol/NH_4OH/H_2O mixture (8:1:1) for the reactions using ^3H or a 2-propanol/NH_4OH/H_2O mixture (6:0.2:3.8) for those using ^{32}P.

For assays employing [^{3}H]FPP, the ^{3}H-labeled product and the unreacted [^{3}H]FPP were located by autoradiography following fluorographic enhancement (En^{3}Hance, NEN Life Sciences), the corresponding regions were cut out from the plate, and the amount of radioactivity was determined. For assays employing the [^{32}P]FPP, $^{32}PP_i$ and unreacted [^{32}P]-FPP were visualized and quantified by phosphoimager analysis. Product formation was quantified from the ratio of radioactivity in the product to the total radioactivity. Initial velocities were determined using the linear relationship $P(t) = V_{int}t$. The initial velocities were plotted versus the peptide concentration, and the results were fit to eq 4:

$$V_{int} = \frac{k_{cat}[E]_{tot}[S]}{[S] + K_m} \quad (4)$$

where $[E]_{tot}$ is the concentration of total enzyme and [S] is the concentration of the peptide substrate.

Single-Turnover and Burst Experiments. A rapid chemical quench flow instrument (KinTek, State College, PA) was used for the single-turnover and pre-steady-state experiments. Enzyme (0.8 μM) and [^{3}H]FPP (0.75 μM) were added to the same assay buffer used in the steady-state experiments (see above) at 25 °C for >15 min to preform the E·FPP complex. For the single-turnover experiments, the E·FPP complex was rapidly mixed with an equal volume (15 μL) of the peptide substrate, as indicated in the appropriate figure legend. Reactions were quenched at the specified times by addition of 1 M HCl in 80% 2-propanol. To prevent hydrolysis of the unreacted FPP, the mixture whose reaction had been quenched was immediately neutralized with NaOH. Aliquots (60 μL) of the final solution were spotted onto the preabsorbent zone of glass-backed TLC plates (silica gel 60), and the plates were developed with a 2-propanol/NH_4OH/H_2O mixture (8:1:1). Plates were then exposed to film for 36−48 h following fluorographic enhancement, and using the fluorograph as a guide, the product and FPP bands were scraped from the plate for radioactivity quantitation. Product formation was assessed by ratio analysis as described above.

Single-turnover data were fit with KaleidaGraph (Synergy Software) or Systat (Systat, Inc.). The chemical rate constants were approximated by single-exponential fits (eq 5) of the time course for the appearance of the product at saturating enzyme concentrations using KaleidaGraph and eq 5:

$$[P]_t = [FPP]_0(1 - e^{-k_{obs}t}) \quad (5)$$

where $[P]_t$ is the concentration of the product at time t, $[FPP]_0$ is the initial concentration of FPP, and k_{obs} is the observed rate constant for product formation. This fit is ideal for reactions in which the peptide dissociation rate constant is faster than the chemical rate constant such that the bound E·FPP·peptide complex equilibrates rapidly with the E·FPP complex and the peptide before it is converted to enzyme and product. Under these conditions, values for k_{chem}, the rate constant for the chemical step, and $K_{1/2}$ can be determined with a hyperbolic fit (eq 6) of the observed rate constants over a range of enzyme concentrations.

$$k_{obs} = \frac{k_{chem}[Pep]}{[Pep] + K_{1/2}} \quad (6)$$

For any reaction in which the chemical rate constant is significantly faster than the peptide dissociation rate constant, the enzyme−substrate complex does not equilibrate rapidly with the free enzyme and peptide. Such a reaction mechanism is best fit by two consecutive irreversible single-exponential equations where k_1 reflects peptide association and k_{chem} reflects the rate constant for the chemical step (eq 7, Systat).

$$[P]_t = [FPP]_0\left[1 + \left(\frac{1}{k_1[Pep] - k_{chem}}\right)(k_{chem}e^{-k_1[Pep]t} - k_1[Pep]e^{-k_{chem}t})\right] \quad (7)$$

However, at very low or high peptide concentrations, the association rate constant or chemical rate constant, respectively, can be estimated by a single-exponential fit of the time course for the appearance of the product (eq 5).

RESULTS

Previous studies led to the conclusion that Tyr361 in the β subunit of FTase was a critical residue involved in protein substrate selectivity and that conversion of this Tyr to Leu was sufficient to convert FTase into an enzyme that prefers to catalyze the farnesylation of a protein that would normally be a substrate for GGTase-I (i.e., a CaaX protein whose C-terminal residue is a Leu) (*29*, *32*). To explore the role of this specific Tyr in the enzymatic mechanism of FTase, in particular, the proposed role for a Leu substitution at this position in protein substrate selectivity, Tyr361 in rat FTase was subjected to site-directed mutagenesis to convert it to Leu, and kinetic analyses were performed on the Y361L mutant enzyme.

Initial Characterization and Steady-State Analysis. Expression of theY361L variant of the FTase β subunit with a wild-type α subunit in *Escherichia coli* produced a recombinant mutant enzyme that was purified as a heterodimer and whose purification profile was similar to that of wild-type FTase (not shown), indicating that the mutant enzyme was correctly folded. Proper folding of the mutant enzyme was also indicated by the finding that the equilibrium dissociation constant for FPP binding by the Y361L variant (data not shown) was essentially identical to that determined for the wild-type enzyme (i.e., ~5 nM) (*24*). These data indicated that the Leu-for-Tyr substitution at this position did not have any significant effect on enzyme stability or the binding of FPP.

In the first series of experiments to probe the kinetic mechanism of the Y361L variant, the steady-state parameters K_m and k_{cat} were examined. Two different peptides were used

Table 1: Kinetic Parameters for Wild-Type and Y361L FTase[a]

	GCVLS		TKCVIL	
	WT	Y361L	WT	Y361L
k_{cat} (min^{-1})	3.3 ± 0.9	<0.07[b]	5.9 ± 0.8	3.7 ± 0.6
$K_{m,pep}$ (μM)	0.6 ± 0.7	nd	59.9 ± 4.5	10.7 ± 1.9
k_{cat}/K_m (min^{-1} μM^{-1})	6.0	nd	9.9×10^{-2}	3.4×10^{-1}
k_{pr} (min^{-1})[c]	1.8	<0.06	9	4.5
K_d (μM)	0.21 ± 0.08	0.005 ± 0.002	>500[d]	>500[d]
k_{chem} (s^{-1})	12[e]	9.6 ± 0.4	>1.5[d]	>0.8[d]
$K_{1/2}$ (μM)	20[e]	21.5	>300[d]	>300[d]
k_1 (M^{-1} s^{-1})	6×10^5[e]	$(6.1 \pm 0.3) \times 10^5$	$>1.6 \times 10^3$[d]	$>5.6 \times 10^3$[d]

[a] Kinetic values were determined for wild-type (WT) and Y361L FTase with peptides GCVLS and TKCVIL. The steady-state values are averages of three separate determinations. The term nd means that the value could not be determined. [b] Less than 10% product formation was observed over 2.5 h. [c] The rate constants for product release, k_{pr}, were calculated from the equation $k_{cat} = k_{chem}k_{pr}/(k_{chem} + k_{pr})$. [d] These values represent lower limit estimates due to limitations in the concentration of TKCVIL that could be used in the assays. The k_1 values were calculated from k_{cat}/K_m. [e] These values were taken from ref *24*.

as substrates: GCVLS, which corresponds to the C-terminus of the prototypical FTase substrate H-Ras, and TKCVIL, a preferred substrate of GGTase-I. The data obtained from this steady-state analysis are summarized in Table 1 and are consistent with previous findings that the catalytic efficiency, k_{cat}/K_m, of wild-type FTase is much greater with GCVLS as a substrate than with TKCVIL (*29*, *32*). In these steady-state studies, theY361L variant catalyzed farnesyl transfer to the TKCVIL peptide slightly more efficiently than did the wild-type enzyme; however, essentially no activity was observed with the Y361L mutant when GCVLS was used as the substrate. Similar results were observed when full-length protein substrates (bacterially expressed H-Ras protein or alternatively an H-Ras protein whose C-terminal amino acid residue had been changed to a Leu, H-Ras-CVLL) were used in the assay (data not shown). Therefore, as reported previously, under steady-state conditions the Y361L variant appears to prefer the GGTase-I peptide substrate over that of a FTase substrate sequence. Hence, in the absence of further analysis, one would conclude, as did the group performing the initial characterization of this mutant enzyme (*29*), that the recognition of CaaX sequences by FTase was altered by the Y361L mutation.

Measurement of Peptide Affinities. Kinetic evaluation of FTase is complicated by the fact that product dissociation is the rate-limiting step for steady-state turnover by the enzyme (*23*). Hence, it was considered important to directly examine peptide binding affinities to determine if Y361L was in fact deficient in its ability to recognize GCVLS while having an increased affinity for TKCVIL. To obtain these data, we took advantage of a fluorescence resonance energy transfer method for direct measurement of the affinity of peptide substrates binding to an E·isoprenoid binary complex that was recently developed (*37*). An inactive E·isoprenoid complex with the Y361L mutant was formed by preincubating the mutant enzyme with the FPP analogue *I*. The fluorescence increase resulting from titration of dansyl-GCVLS into a solution of the Y361L·*I* complex is shown in Figure 2A. Surprisingly, this analysis yielded a K_d value of 0.012 μM, an affinity even higher than that of 0.21 ± 0.08 μM determined for the wild-type enzyme (data not shown). To confirm that the dansyl group itself did not perturb the affinity measurement, a competition assay was performed; the data that were obtained showed that the binding affinity of the unmodified GCVLS (0.005 μM) was essentially the same as that of the dansylated form (Figure 2B). These results indicate that the Y361L mutation increases, rather than decreases, the affinity of this particular FTase peptide substrate.

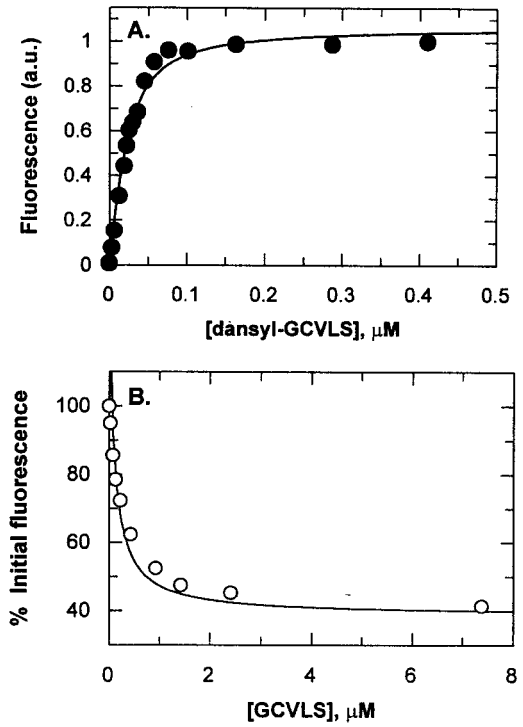

FIGURE 2: Peptide binding by the FTase Y361L variant. (A) Binding of a dansyl-labeled peptide. The Y361L variant of FTase (0.02 μM) was preincubated with the FPP analogue *I* (0.2 μM) at 25 °C. Dansyl-GCVLS was titrated into this solution, and emission of the dansyl group was monitored at 496 nm after excitation by energy transfer from the enzyme whose Trp residues were excited at 280 nm. The dansyl-GCVLS fluorescence was corrected by subtracting the signal from the addition of dansyl-GAVLS to the enzyme complex. The resulting curve was fit to eq 2 and yielded a K_d of 0.012 ± 0.002 μM. (B) Competition assay. Dansyl-GCVLS (0.25 μM) was added to a solution of Y361L·*I* prepared as above to form the Y361L·*I*·dansyl-GCVLS ternary complex. Titration of this solution with increasing concentrations of the GCVLS peptide resulted in a fluorescence decrease. These data were fit to eq 3 to obtain a K_d for GCVLS of 0.005 ± 0.002 μM.

The second surprise from these peptide substrate binding experiments came from analysis of the binding of the TKCVIL peptide. All attempts to compete binding of dansyl-GCVLS to either the wild-type or Y361L FTase with increasing concentrations of TKCVIL yielded no significant

Scheme 1: Kinetic Scheme for FTase[a]

$$E + FPP \rightleftharpoons E{\cdot}FPP + Pep \underset{k_{-1}}{\overset{k_1}{\rightleftharpoons}} E \begin{matrix}{\cdot}FPP \\ {\cdot}Pep\end{matrix} \xrightarrow{k_{chem}} E \begin{matrix}{\cdot}PP_i \\ {\cdot}F\text{-}Pep\end{matrix} \overset{k_{cat}}{\rightleftharpoons} E + F\text{-}Pep + PP_i$$

[a] For this scheme, k_1 denotes the peptide association rate constant, k_{-1} is the peptide dissociation rate constant, and k_{chem} represents the rate constant for the chemical step. Under steady-state conditions, k_{cat} is a measure of product release (*23*).

fluorescence changes using peptide concentrations as high as 120 μM (data not shown), indicating that the TKCVIL peptide binds very weakly (K_d > 500 μM; calculated by assuming <20% formation of the E·*I*·TKCVIL complex at the highest concentration of peptide) to both the wild-type and mutant enzymes. These results indicate that, in direct contrast to what would be expected on the basis of the steady-state results (see above), CaaX peptide recognition by the Y361L variant is unchanged from that of wild-type FTase.

Single-Turnover Studies. Once it was clear that the apparently altered CaaX substrate utilization by the Y361L variant was not due to alterations in recognition of substrate peptides, our approach shifted to the use of single-turnover and pre-steady-state kinetics to examine the individual steps in the reaction (see Scheme 1) with the hope of determining the underlying mechanism of the altered activity. Since the rate constant of product formation for FTase is ~200-fold faster than the steady-state k_{cat} value (*17*, *23*, *24*), k_{cat} is not a measure of the chemical step but rather corresponds to the rate of product release from the enzyme. The initial goal of these studies was to determine whether the discrepancy between peptide substrate recognition and turnover for the Y361L variant could be explained by an alteration in the chemical step, k_{chem}, in the farnesylation reaction. To compare the kinetics of the single-turnover reaction of the Y361L variant with that of the wild-type FTase, GCVLS was used as the peptide substrate under conditions in which only one turnover of the enzyme was allowed. Time courses of product formation at each concentration of GCVLS were fit to a single-exponential equation (eq 5). The dependence of the observed rate constant for product formation on peptide concentration was then fit to a hyperbolic equation (eq 6) that assumed a rapid equilibrium mechanism of peptide binding to the E·FPP complex. The resulting $K_{1/2}$ of 21.5 μM (data not shown) was significantly greater than the affinity determined through the use of fluorescent experiments (see above), indicating that the $K_{1/2}$ for the single turnover is not equal to the equilibrium dissociation for peptide binding to the E·FPP complex. Thus, as in the case of the wild-type enzyme (*24*), the kinetic mechanism for the Y361L mutant does not reflect a rapid equilibrium binding of the peptide.

We next analyzed the single-turnover data via a model, including two consecutive irreversible steps for peptide binding and product formation. With this mechanism, the pseudo-first-order rate constant can be estimated at very low peptide concentrations by fitting the data to a single-exponential equation. The second-order rate constant for peptide binding to the E·FPP complex can then be estimated from the slope of a plot of the observed rate constant for product formation, k_{obs}, versus peptide concentration (*39*). Using this approach, the association rate constant, k_1, for GCVLS binding to the Y361L·FPP complex was estimated to be 1×10^6 M^{-1} s^{-1}, a value slightly larger than 6×10^5 M^{-1} s^{-1} measured for the wild-type enzyme (*24*) (Table 1). An approximation of the actual rate constant of product formation, k_{chem}, of 8 s^{-1} was obtained from single-exponential fits at high peptide concentrations; this value was again comparable to the value of 12 s^{-1} previously determined for the wild-type enzyme (*24*) (Table 1). Furthermore, a three-dimensional fit of the time courses for the appearance of the product at various concentrations of peptide (Figure 3) using the equation describing two consecutive irreversible reactions (eq 7) yielded the following similar values: $k_{chem} = 9.6 \pm 0.4$ s^{-1} and $k_1 = (6.1 \pm 0.3) \times 10^5$ M^{-1} s^{-1} (Table 1). These results indicate that the Y361L mutant binds and catalyzes the farnesylation of the peptide substrate GCVLS as efficiently as the wild-type FTase and, furthermore, that it follows a similar kinetic pathway. These findings are a marked contrast to both the previous studies (*29*, *32*) and our steady-state results described above in which it appeared that the Y361L variant was greatly impaired in its ability to recognize and act on preferred substrates of FTase.

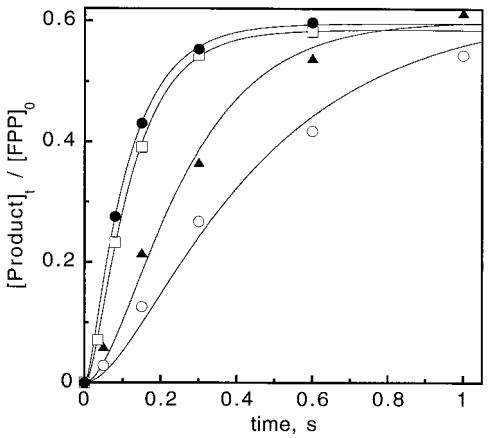

FIGURE 3: Single-turnover reaction of the FTase Y361L variant as a function of peptide concentration. The Y361L variant (0.8 μM) was preincubated with [^{3}H]FPP (0.75 μM) at 25 °C for >15 min. The reaction was initiated by the rapid addition of an equal volume of buffer containing the GCVLS peptide. Reactions were quenched by the addition of 1 M HCl in 80% 2-propanol and the mixtures immediately neutralized with NaOH, and the level of product formation was determined as described in Experimental Procedures. The peptide concentrations are 5 (○), 10 (▲), 50 (□), and 100 μM (●). Because the enzyme mechanism proceeds through two consecutive steps for peptide binding and product formation when using GCVLS as a peptide substrate, the association [$k_1 = (6.1 \pm 0.3) \times 10^5$ M^{-1} s^{-1}] and product formation ($k_{chem} = 9.6 \pm 0.4$ s^{-1}) rate constants were determined using a three-dimensional fit of the data for the appearance of product as a function of time using eq 7.

The single-turnover experiments with the wild-type and mutant enzymes were also performed using the GGTase-I peptide substrate, TKCVIL. Because the K_d measurements by fluorescence suggested a weak binding of TKCVIL to either enzyme, we assumed a rapid equilibrium binding in which the rate of peptide dissociation from the ternary complex (E·FPP·peptide) is much greater than the maximum rate constant of product formation, k_{chem}. Once again, wild-type FTase and the Y361L variant behaved similarly. Consistent with the weak interaction detected in the direct binding studies, saturation of the observed rate constant for product formation was not reached even at TKCVIL concentrations as great as 1 mM (Figure 4). A hyperbolic

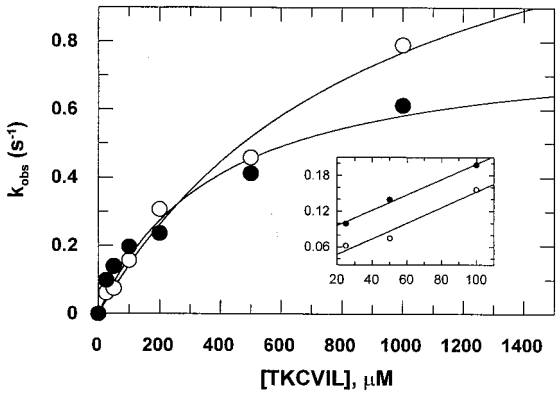

FIGURE 4: Pre-steady-state analysis of TKCVIL utilization by wild-type FTase and the Y361L variant. Experiments were performed with either wild-type FTase (○) or the Y361L variant (●) as described in the legend of Figure 3 except TKCVIL was used as the peptide substrate. The rapid equilibrium mechanism followed by FTase when TKCVIL is used as the peptide substrate allows a hyperbolic fit of the data (eq 6), yielding estimates for k_{chem} of 1.5 and 0.8 s^{-1} for the wild type and the Y361L variant, respectively. The inset shows the linear dependence of the observed rate constant for product formation, k_{obs}, at low TKCVIL concentrations. The slope of the line gives a k_1 value of $(1.3 \pm 0.3) \times 10^3$ M^{-1} s^{-1} for association of TKCVIL with either enzyme, which is consistent with the lower limits for k_1 calculated from k_{cat}/K_m (Table 1).

fit of the data indicates a k_{-1}/k_1 value for TKCVIL of 1.2 mM for wild-type FTase and a slightly smaller value of 0.6 mM for the Y361L mutant. Since, for a rapid equilibrium binding mechanism, the value of $K_{1/2}$ in this single-turnover experiment directly reflects the peptide affinity of the E·FPP complex (*39*), these data clearly demonstrate that the affinity of Y361L for the TKCVIL peptide is increased at most 2-fold. Additionally, the maximum rate constant of product formation was only $\sim$1 s^{-1} for both the wild-type and Y361L enzymes, further demonstrating that TKCVIL is a poor substrate for either enzyme. The dependence of k_{obs} on low TKCVIL concentrations yielded a second-order rate constant of 1.3×10^3 M^{-1} s^{-1} with either enzyme, which is consistent with lower limit estimates for the association rate constant of TKCVIL with FTase derived from k_{cat}/K_m (Table 1). For this peptide, both the K_d and $K_{1/2}$ are increased significantly and the k_{chem} is decreased, suggesting that the peptide binding equilibrium mechanism is correct for the single-turnover data. However, the k_{chem} and $K_{1/2}$ values estimated from these data are still larger than k_{cat} and K_m, respectively. This suggests that, for the TKCVIL peptide, product dissociation remains the main rate-contributing step for k_{cat} and K_m does not reflect K_d. The modest increase in the affinity of TKCVIL observed for the Y361L mutant may also be reflected in the modestly decreased k_{cat} observed for the mutant enzyme with this substrate (Table 1).

The equilibrium peptide affinity and single-turnover results presented thus far indicate that wild-type FTase and the Y361L variant follow similar kinetic pathways for the binding and catalysis of peptide substrates. Furthermore, these results show that both enzymes recognize and catalyze efficient farnesyl transfer to the FTase-preferred peptide substrate GCVLS, yet both are much less efficient at utilizing TKCVIL, which is a preferred substrate of GGTase-I. These results beg the question as to why product formation was not observed in the steady-state analysis of the Y361L mutant when the GCVLS peptide was used as the substrate, since this mutant enzyme not only clearly binds this peptide substrate but also catalyzes farnesylation in a single turnover as efficiently as the wild-type enzyme. At this point, it became clear that the answer almost assuredly must lie with the product release step.

Examination of Product Dissociation. Steady-state analysis utilizes rate measurements based on multiple turnovers, and hence, the measured k_{cat} cannot be greater than the rate-limiting step(s) in the reaction pathway, which for wild-type FTase is product release. Hence, the findings described in detail above that the Y361L mutant binds the GCVLS peptide substrate and catalyzes the farnesylation of this peptide in a manner similar to the wild-type enzyme suggested that the apparent inability, or greatly reduced ability, of the Y361L variant to process GCVLS in a steady-state situation was likely due to some defect in product release. Hence, an analysis of the product dissociation step in the reaction catalyzed by the Y361L mutant was undertaken.

Product release by wild-type FTase and the Y361L variant was examined by use of an experimental approach that combined single-turnover and steady-state measurements. As with the single-turnover experiments described above, stoichiometric amounts of enzyme and [^{3}H]FPP were preincubated in one syringe of the rapid quench instrument. This E·FPP solution was then rapidly mixed with GCVLS alone to initiate a single turnover, or alternatively, the E·FPP complex was mixed with GCVLS and an excess of FPP, which would allow multiple turnovers of the enzyme. In the absence of excess FPP, the time dependence of product formation could be fit to a single-exponential equation (eq 5) that yielded a rate constant of approximately 7 s^{-1} [Figure 5A,B (○)]; this maximum rate constant of product formation is consistent with the aforementioned value of k_{chem}. As expected, the addition of excess FPP in the reaction mixture for the wild-type enzyme resulted in a burst of product formation followed by a slower linear phase [Figure 5A (●)] corresponding to a rate constant for product release, k_{pr}, of 1.8 min^{-1} calculated from the equation $k_{cat} = k_{chem}k_{pr}/(k_{chem} + k_{pr})$ (Table 1). The fast phase corresponds to the first turnover of the enzyme, and the slow linear phase represents the steady-state turnover limited by product release. Most importantly, this steady-state phase was not observed with the Y361L variant subjected to the same type of analysis [Figure 5B (●)]. In fact, multiple turnovers were not detected even after incubation for 1 h (data not shown), indicating that the mutant is incapable of multiple turnovers. Hence, when the GCVLS peptide is used as a substrate in the farnesylation reaction catalyzed by the Y361L mutant, the affinity of the peptide and the product formation step are not altered, but rather, it is the product release step which is inhibited and impedes a second turnover. The small amount of enzyme relative to the saturating concentrations of substrates used in the steady-state assays accounts for the lack of observable activity under these conditions.

DISCUSSION

FTase catalyzes the posttranslational modification of several proteins involved in cellular proliferation, and this enzyme has emerged as a major target for development of cancer therapeutics (*40*). Additionally, the finding that geranylgeranylation of CaaX-type proteins are important in cell cycle progression and proliferation has increased interest

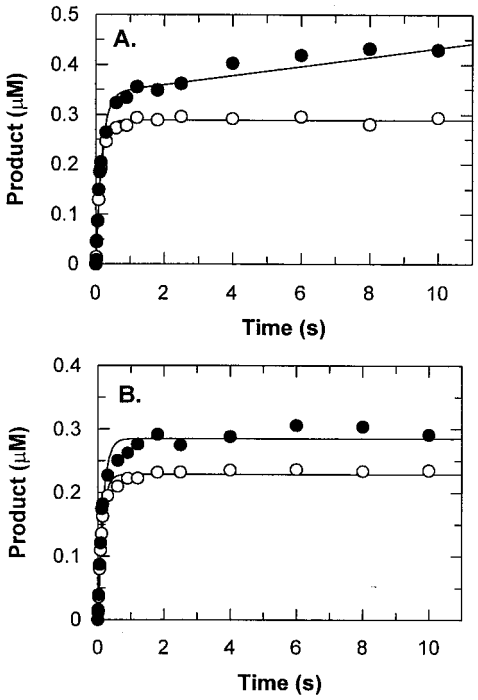

FIGURE 5: Analysis of the abilities of wild-type FTase and the Y361L variant to catalyze multiple turnovers. The ability of the enzymes to catalyze multiple turnovers was assessed by measuring the activity in the presence and absence of excess FPP. Wild-type FTase or the Y361L variant, both at 0.75 μM, were mixed with an equimolar amount of [^{3}H]FPP to preform the respective E·FPP complexes. These binary complexes were then rapidly mixed with 500 μM GCVLS in the absence or presence of additional [^{3}H]FPP. (A) Catalysis by wild-type FTase. In the absence of excess FPP (○), the data were fit to a single-exponential equation (eq 5), yielding a k_{chem} of 7.4 ± 0.3 s^{-1}. In the presence of excess FPP, (●) the k_{chem} was determined to be 5.9 ± 0.4 s^{-1} (eq 7); in this case, the rate constant of the linear phase was estimated to be 0.026 ± 0.003 s^{-1}. (B) Catalysis by the Y361L variant. Both curves are single-exponential fits of the data (eq 5); k_{chem} was determined to be 7.7 ± 0.4 s^{-1} in either the absence (○) or presence (●) of FPP.

in development of specific inhibitors of the close relative of FTase that is responsible for this modification, i.e., GGTase-I (*41*). FTase in particular has become a major subject of structural and structure−function analyses as part of a widespread program to develop selective inhibitors. To date, however, a limited number of residues have been implicated as being involved in protein substrate recognition, with the most studied being a specific Tyr residue in the β subunit corresponding to Y361 in mammalian FTase (*29*, *32*). In our study, direct binding measurements and transient kinetic methods were employed to more fully evaluate the role of Y361 in substrate recognition and catalysis by mammalian FTase.

The initial findings in this study were similar to those in previous reports on the analysis of this mutant in that, under steady-state conditions, the Y361L mutant did not appear to catalyze the farnesylation of a protein or peptide substrate whose CaaX sequence marks it as a substrate of FTase. In contrast, when a protein or peptide containing a C-terminal Leu residue (i.e., the CaaX sequence preferred by GGTase-I) was used as a substrate, the Y361L mutant exhibited measurable catalytic activity. Hence, when examined under steady-state conditions, the introduction of a single mutation in the β subunit at position 361 appeared to have switched the protein substrate selectivity of FTase to resemble that of GGTase-I.

A much different picture for the Y361L mutant emerged, however, when direct binding of peptide substrates was examined (Figure 2). These studies revealed that the Y361L variant, rather than having diminished affinity for GCVLS, retained high-affinity binding of this normal peptide substrate and that the K_d value of 5 nM was actually 40-fold tighter than that for the wild-type enzyme. In contrast, the binding of the "GGTase-I substrate", i.e., the TKCVIL peptide, to either the wild type or the Y361L variant was very weak.

To sort out the apparent contradiction between the steady-state kinetic and direct binding results in terms of peptide substrate recognition and/or utilization by the Y361L variant of FTase, single-turnover and pre-steady-state techniques were employed. The single-turnover experiments (Figure 3) clearly demonstrated that the Y361L mutant enzyme efficiently catalyzed the farnesylation of GCVLS with a maximum rate constant of product formation that was essentially equal to that of the wild-type enzyme, indicating that no significant alteration of the chemical step had occurred in the mutant. Repeating the single-turnover experiments with TKCVIL as the peptide substrate yielded similar k_{chem} values of ~1 s^{-1} and $K_{1/2}$ values of >300 μM for both wild-type and the Y361L variant. Hence, both the equilibrium binding and pre-steady-state results showed that the Y361L mutant had not switched substrate selectivity.

While the Y361L mutant behaved in a manner very similar to that of the wild-type enzyme in the single-turnover studies, the steady-state results provided much different pictures of the two enzymes. The apparent discrepancies between the two approaches could be explained, however, by a mechanism in which the Y361L variant was able to catalyze a single turnover of the GCVLS peptide but was then unable to release product from the enzyme. The absence of a steady-state phase following the single turnover for Y361L [Figure 5B (●)] showed that the release of product, farnesyl-GCVLS, was inhibited for this variant. Hence, although Y361L catalyzed a single turnover in the steady-state assays, the very small amount of enzyme used for these types of assays precluded detection of the product and little or no apparent activity was observed.

The direct binding measurements and pre-steady-state kinetics presented here indicate Y361 in the β subunit of FTase is not significantly involved in peptide substrate selection, but rather that substitutions at this position can dramatically influence product release from the enzyme. Although the ternary complex structures of FTase determined to date do not provide clues as to why a mutation at position 361 in the β subunit should produce such a major alteration in product dissociation, it seems likely that interactions of the substrate peptide with the enzyme are affected that contribute to both the tight binding of the GCVLS substrate and subsequent release of the farnesylated peptide product following catalysis. A structure of the FTase·product complex could provide additional insight into the mechanism of, and the potential role of Y361 in, these processes. We anticipate that such structural determinations, together with information provided by additional structure−function studies, will facilitate the design of specific, tight-binding inhibitors of FTase.

ACKNOWLEDGMENT

We thank Ruth Fu and Chih-chin Huang for helpful comments and discussions during the course of this work, Ken Keller for assistance in the synthesis of [^{32}P]FPP, and Carolyn Weinbaum for technical assistance.

REFERENCES

1. Zhang, F. L., and Casey, P. J. (1996) *Annu. Rev. Biochem. 65*, 241.
2. Hightower, K. E., and Fierke, C. A. (1998) *Curr. Opin. Chem. Biol. 3*, 176.
3. Sinensky, M. (2000) *Biochim. Biophys. Acta 1484*, 93.
4. Glomset, J. A., and Farnsworth, C. C. (1994) *Annu. Rev. Cell Biol. 10*, 181.
5. Parish, C. A., and Rando, R. R. (1996) *Biochemistry 35*, 8473.
6. Hancock, J. F., Magee, A. I., Childs, J. E., and Marshall, C. J. (1989) *Cell 57*, 1167.
7. Schafer, W. R., and Rine, J. (1992) *Annu. Rev. Genet. 25*, 209.
8. Casey, P. J., and Seabra, M. C. (1996) *J. Biol. Chem. 271*, 5289.
9. Casey, P. J., Thissen, J. A., and Moomaw, J. F. (1991) *Proc. Natl. Acad. Sci. U.S.A. 88*, 8631.
10. Yokoyama, K., Goodwin, G. W., Ghomashchi, F., Glomset, J. A., and Gelb, M. H. (1991) *Proc. Natl. Acad. Sci. U.S.A. 88*, 5302.
11. Reiss, Y., Goldstein, J. L., Seabra, M. C., Casey, P. J., and Brown, M. S. (1990) *Cell 62*, 81.
12. Chen, W.-J., Andres, D. A., Goldstein, J. L., Russell, D. W., and Brown, M. S. (1991) *Cell 66*, 327.
13. Zhang, F. L., Diehl, R. E., Kohl, N. E., Gibbs, J. B., Giros, B., Casey, P. J., and Omer, C. A. (1994) *J. Biol. Chem. 269*, 3175.
14. Reiss, Y., Brown, M. S., and Goldstein, J. L. (1992) *J. Biol. Chem. 267*, 6403.
15. Chen, W.-J., Moomaw, J. F., Overton, L., Kost, T. A., and Casey, P. J. (1993) *J. Biol. Chem. 268*, 9675.
16. Moomaw, J. F., and Casey, P. J. (1992) *J. Biol. Chem. 267*, 17438.
17. Huang, C.-C., Casey, P. J., and Fierke, C. A. (1997) *J. Biol. Chem. 272*, 20.
18. Park, H.-W., Boduluri, S. R., Moomaw, J. F., Casey, P. J., and Beese, L. S. (1997) *Science 275*, 1800.
19. Long, S. B., Casey, P. J., and Beese, L. S. (1998) *Biochemistry 37*, 9612.
20. Strickland, C. L., Windsor, W. T., Syto, R., Wang, L., Bond, R., Wu, Z., Schwartz, J., Le, H. V., Beese, L. S., and Weber, P. C. (1998) *Biochemistry 37*, 16601.
21. Long, S. B., Casey, P. J., and Beese, L. S. (2000) *Structure 8*, 209.
22. Pompliano, D. L., Schaber, M. D., Mosser, S. D., Omer, C. A., Shafer, J. A., and Gibbs, J. B. (1993) *Biochemistry 32*, 8341.
23. Furfine, E. S., Leban, J. J., Landavazo, A., Moomaw, J. F., and Casey, P. J. (1995) *Biochemistry 34*, 6857.
24. Huang, C.-C., Hightower, K. E., and Fierke, C. A. (2000) *Biochemistry 39*, 2593.
25. Tschantz, W. R., Furfine, E. S., and Casey, P. J. (1997) *J. Biol. Chem. 272*, 9989.
26. Dolence, J. M., Rozema, D. B., and Poulter, C. D. (1997) *Biochemistry 36*, 9246.
27. Kral, A. M., Diehl, R. E., deSolms, S. J., Williams, T. M., Kohl, N. E., and Omer, C. A. (1997) *J. Biol. Chem. 272*, 27319.
28. Goodman, L. E., Judd, S. R., Farnsworth, C. C., Powers, S., Gelb, M. H., Glomset, J. A., and Tamanoi, F. (1990) *Proc. Natl. Acad. Sci. U.S.A. 87*, 9665.
29. Del Villar, K., Mitsuzawa, H., Yang, W., Sattler, I., and Tamanoi, F. (1997) *J. Biol. Chem. 272*, 680.
30. Trueblood, C. E., Boyartchuk, V. L., and Rine, J. (1997) *Proc. Natl. Acad. Sci. U.S.A. 94*, 10774.
31. Wu, Z., Demma, M., Strickland, C. L., Radisky, E. S., Poulter, C. D., Le, H. V., and Windsor, W. T. (1999) *Biochemistry 38*, 11239.
32. Del Villar, K., Urano, J., Guo, L., and Tamanoi, F. (1999) *J. Biol. Chem. 274*, 27010.
33. Keller, R. K., and Thompson, R. (1993) *J. Chromatogr. 645*, 161.
34. Ellman, G. L. (1959) *Arch. Biochem. Biophys. 82*, 70.
35. Fu, H.-W., Beese, L. S., and Casey, P. J. (1998) *Biochemistry 37*, 4465.
36. Zimmerman, K. K., Scholten, J. D., Huang, C.-C., Fierke, C. A., and Hupe, D. (1998) *Protein Expression Purif. 14*, 395.
37. Hightower, K. E., Huang, C.-C., Casey, P. J., and Fierke, C. A. (1998) *Biochemistry 37*, 15555.
38. Segel, I. H. (1975) in *Enzyme Kinetics*, Wiley-Interscience, New York.
39. Fierke, C. A., and Hammes, G. G. (1995) *Methods Enzymol. 249*, 3.
40. Gibbs, J. B., and Oliff, A. (1997) *Annu. Rev. Pharmacol. Toxicol. 37*, 143.
41. Vasudevan, A., Qian, Y., Vogt, A., Blaskovich, M. A., Ohkanda, J., Sebti, S. M., and Hamilton, A. D. (1999) *J. Med. Chem. 42*, 1333.

BI001084R